Bioresource Technology 181 (2015) 13–17

Contents lists available at ScienceDirect

Bioresource Technology

journal homepage: www.elsevier.com/locate/biortech

Manganese oxide-modified biochars: Preparation, characterization, and sorption of arsenate and lead

Shengsen Wang [a,b], Bin Gao [c,*], Yuncong Li [a,b], Ahmed Mosa [d], Andrew R. Zimmerman [e], Lena Q. Ma [b], Willie G. Harris [b], Kati W. Migliaccio [a,c]

[a] Tropical Research and Education Center, University of Florida, Homestead, FL 33031, United States
[b] Soil and Water Science Department, University of Florida, Gainesville, FL 32611, United States
[c] Department of Agricultural and Biological Engineering, University of Florida, Gainesville, FL 32611, United States
[d] Soils Department, Faculty of Agriculture, Mansoura University, 35516 Mansoura, Egypt
[e] Department of Geological Sciences, University of Florida, Gainesville, FL 32611, United States

HIGHLIGHTS

- Two modification methods were used to improve biochar's sorption ability.
- MPB and BPB sorbed more As and Pb than the unmodified biochar.
- BPB showed the highest sorption enhancement.
- Birnessite particles within BPB promoted heavy metal sorption.

ARTICLE INFO

Article history:
Received 10 November 2014
Received in revised form 5 January 2015
Accepted 9 January 2015
Available online 17 January 2015

Keywords:
Biochar
Birnessite
MnO
Nanocomposite
Adsorption

ABSTRACT

This work explored two modification methods to improve biochar's ability to sorb arsenic (As) and lead (Pb). In one, pine wood feedstock was pyrolyzed in the presence of $MnCl_2{\cdot}4H_2O$ (MPB) and in the other it was impregnated with birnessite via precipitation following pyrolysis (BPB). The resulting biochars were characterized using thermogravimetry, X-ray diffraction, X-ray photoelectron spectroscopy, scanning electron microscopy, and energy-dispersive X-ray analyses. The dominant crystalline forms of Mn oxides in the MPB and BPB were manganosite and birnessite, respectively. Batch sorption studies were carried out to determine the kinetics and magnitude of As(V) and Pb(II) onto the biochars. As(V) and Pb(II) sorption capacities of MPB (0.59 and 4.91 g/kg) and BPB (0.91 and 47.05 g/kg) were significantly higher than that of the unmodified biochar (0.20 and 2.35 g/kg). BPB showed the highest sorption enhancement because of the strong As(V) and Pb(II) affinity of its birnessite particles.

1. Introduction

Reclamation of heavy metals via adsorption is a convenient and prevailing approach to remove heavy metals, such as arsenic (As) and lead (Pb) from wastewater (Zhang et al., 2010). Recently, research has been directed at producing and optimizing adsorbent materials that have characteristics similar to activated carbon (C) materials but are more cost efficient and environmentally friendly (Inyang et al., 2010). For example, biochar is pyrogenic C produced by thermal conversion of lignocellulose biomass under oxygen-free or limited conditions (Lehmann et al., 2006; Sun et al., 2014). Biochar has been recognized as a candidate sorbent for As and Pb (Inyang et al., 2011; Mohan et al., 2007). However, the As and Pb sorption capacities of most of the pristine biochars are lower than some commercial or modified adsorbents (Zhang et al., 2013; Zhou et al., 2014). Thus, the goal of this research was to enhance sorption capacity of biochar by producing biochar-based composites.

Manganese (Mn) oxide minerals are commonly found in soil, especially those that have undergone cycles of wetting and drying (Essington, 2004; Post, 1999). Of more than thirty Mn-oxides found in terrestrial environments, birnessite is one of the most abundant (O'Reilly and Hochella, 2003; Post, 1999). It has been noted for their high adsorption capacity of both arsenite (As(III)) and arsenate (As(V)) (Lenoble et al., 2004; Manning et al., 2002). In addition, birnessite also has high oxidization potential and can convert As(III) to less toxic As(V) (Lafferty et al., 2010a; Post, 1999). The sorption of As(V) by birnessite is pH dependent, but

* Corresponding author. Tel.: +1 352 392 1864x285.
E-mail address: bg55@ufl.edu (B. Gao).

http://dx.doi.org/10.1016/j.biortech.2015.01.044
0960-8524/

there is only a gradual decrease of sorption between pH 2 and 10 (Zhang and Sun, 2013). This is because surface complexation interactions between As(V) and Mn-oxides may occur at appropriate ambient pH and the oxygen moiety of As(V) displaces a surface hydroxyl group on Mn-oxide to generate an inner-sphere complex (Manning et al., 2002; Zhang and Sun, 2013).

Mn oxides also have a high potential for Pb(II) sorption (Matocha et al., 2001; O'Reilly and Hochella, 2003). Lead sorption was observed to be associated with internal reactive sites. For example, Pb(II) may enter the space within birnessite's layers and tunnel into the internal cryptomelane structure (Lee et al., 2013; O'Reilly and Hochella, 2003).

The specific objectives of this work were to: (1) prepare and characterize two Mn oxide–biochar composites, (2) compare the As(V) and Pb(II) sorption capacities of the composites with that of pristine biochar, and (3) explore the possible mechanisms involved in the As(V) and Pb(II) sorption.

2. Methods

2.1. Reagents

Sodium arsenate dibasic heptahydrate ($Na_2HAsO_4{\cdot}7H_2O$), lead nitrate ($Pb(NO_3)_2$), potassium permanganate ($KMnO_4$), manganese chloride tetrahydrate ($MnCl_2{\cdot}4H_2O$) and concentrated hydrochloric acid (HCl) of analytical grade were purchased from Fisher Scientific and were dissolved in deionized (DI) water (18.2 MΩ) (Nanopure water, Barnstead).

2.2. Sorbent preparation

2.2.1. Mn oxide-modified pine biochar (MPB)

Loblolly pine (*Pinus taeda*) wood was oven dried overnight at 80 °C, then crushed and sieved to obtain the 0.425–1 mm size fraction. After sieving, 14 g of the feedstock was immersed in 100 mL of 5 g L^{-1} $MnCl_2{\cdot}4H_2O$ solution for 2 h. The mixture was oven dried at 80 °C overnight, and then pyrolyzed in a tube furnace (MTI, Richmond, CA) under flowing N_2 by ramping the temperature at a rate of 10 °C per min and holding at a peak temperature of 600 °C for 1 h. Unmodified pine biochar (PB), used as the control treatment, was made similarly but without pre-soaking the feedstock in Mn solution.

2.2.2. Birnessite-modified pine biochar (BPB)

Birnessite was synthesized using a modified $KMnO_4$ precipitation method as described by McKenzie (1980). Briefly, 3.15 g $KMnO_4$ was dissolved in 50 mL DI water, and a 5 g aliquot of PB was added to the solution and agitated for 2 h with a magnetic stirrer. The suspension was then boiled for 20 min, followed by drop wise addition of 3.3 mL concentrated HCl. The reaction was continued for additional 10 min under vigorous stirring. The solution was then allowed to cool to room temperature (22 ± 0.5 °C) and filtered through a 0.22 μm pore size nylon membrane filter. The resulting biochar–birnessite composite was rinsed thoroughly with DI water, oven dried overnight at 80 °C and stored in a closed jar until analysis.

2.3. Sorbent characterization

Total carbon (C), nitrogen (N), and hydrogen (H) content in the biochar samples was analyzed with a CHN elemental analyzer (Carlo-Erba NA-1500). The inorganic element composition of biochar samples was determined according to the AOAC method (AOAC, 1990) and analyzed by inductively coupled plasma–atomic emission spectrometry (ICP–AES, Perkin-Elmer Plasma 3200). Oxygen content was determined by subtracting from 100 the sum of the percentages of all measured elements (C, N, H, and inorganic elements).

Total surface area was measured on a NOVA 1200 analyzer using N_2 sorption Brunauer–Emmett–Teller (BET) method. Scanning electron microscope (SEM) images were obtained on a JEOL JSM-6400 Scanning Microscope. Energy dispersive X-ray fluorescence spectroscopy (EDS, Oxford Instruments Link ISIS) was coupled with SEM in order to map surface elemental distributions and associations in relation to particles embedded in the biochar matrix. Surface elemental composition was also analyzed by X-ray photoelectron spectroscopy (XPS) with a PHI 5100 series ESCA spectrometer (Perkin-Elmer). An X-ray diffractometer (XRD) (Ultima IV X-ray Diffractometer, Rigaku Corporation, Japan) equipped with a stepping motor and graphite crystal monochromator was used to identify Mn bearing crystals. A CuKα radiation source was used, and the scans were made in the 2θ range of 0° and 80°. Thermogravimetric analyses (TGA) of original and modified biochar samples were done using a Mettler Toledo TGA/DSC1 analyzer. The temperature was increased by 10 °C per min between 25 and 700 °C under air atmosphere.

2.4. Adsorption kinetics and isotherm

Investigation of As(V) (10 mg L^{-1}) and Pb(II) (50 mg L^{-1}) sorption kinetics by biochar followed the methods of Zhang et al. (2013). Briefly, around 0.05 g of biochar was added to 20 mL of the sorbate solution in 68 mL digestion vessels (Environmental Express) at room temperature (22 ± 0.5 °C). Thus, sorbent concentrations were about 2.5 g L^{-1} for all treatments. The vessels were placed onto a rotary shaker, and shaken at 40 rpm until sampling. At each sampling time (0, 0.5, 1, 2, 4, 8, 12, 24 and 48 h), the suspensions were immediately filtered through 0.22 μm pore size nylon membrane filters (GE cellulose nylon membrane). As(V) and Pb(II) were measured in the filtrate and sorption was calculated as the difference in initial and final solution concentration of the sorbate.

Adsorption isotherms were determined for these metals using the same procedure as described above but using a range of As(V) (20 mL, 1–20 mg L^{-1}) and Pb(II) (20 mL, 1–300 mg L^{-1}) sorbate solution concentrations and 24 h contact period. The kinetic and isotherm experiments were run in triplicate. The initial pH values of the As(V) and Pb(II) solutions were adjusted to around 7 and 5.5, respectively, with 0.01 M HCl and 0.01 M NaOH.

2.5. Statistical analyses

Modeling of sorption kinetics and isotherm data was conducted with SigmaPlot 12.0 using user-defined functions to minimize the residuals between model-calculated and measured values.

3. Results and discussion

3.1. Sorbent properties

Compared to pristine biochar, bulk C content of MPB and BPB was 6.7% and 24.1% less, respectively (Table 1). Similar trends were also found for Mg, Al, N, and H contents because of the dilution effect. However, the concentration of K in BPB increased several times over the pristine biochar as K was introduced in the synthesis process. Chemical modifications also increased Mn concentrations in MPB and BPB by about 182 and 354 times, respectively, compared to PB (Table 1). These results were confirmed with XPS analysis, which showed that Mn content was 3.7% (atomic) in

Table 1
Elemental composition, surface area and pore volume of pine wood biochar (PB), $MnCl_2{\cdot}4H_2O$ modified biochar (MPB) and biochar modified with synthesized birnessite (BPB).

Biochar	C	N	H	O	Mn	K	Ca	Mg	Al	P	BET surface area $m^2\ g^{-1}$	BJH pore vol (des. leg) cc g^{-1}
	%, mass based											
PB	85.68	0.33	2.13	11.19	0.023	0.052	0.186	0.120	0.041	0.039	209.6	0.003
MPB	78.95	0.26	1.86	14.58	4.19	0.018	0.056	0.062	0.008	0.020	463.1	0.022
BPB	61.54	0.25	1.85	27.65	8.14	0.163	0.246	0.143	0.008	0.012	67.4	0.066

MPB (Fig. S1a, Supporting information) compared to 9.4% (atomic) in BPB (Fig. S1b, Supporting information).

The ash contents of PB, MPB and BPB were 4.02%, 14.0% and 33.4%, respectively (Fig. 1). The higher ash contents of MPB and BPB likely resulted from the addition of Mn oxides. Conversion of PB to MPB resulted in more than a doubling of BET surface area and an increase in pore volume of more than seven times (Table 1). This is likely due to the formation of new Mn-bearing minerals. However, while the pore volume of BPB was 22 times that of PB, the BET surface area decreased by two thirds, suggesting that the birnessite modification may change the pore size distribution of the biochar.

The MPB showed excellent crystallinity (Fig. S2a, Supporting information). Its XRD peaks at d = 2.562, 2.220, 1.570, 1.339, and 1.281 Å correspond to manganosite (MnO) (Chen et al., 2009). The presence of other small XRD peaks may indicate formation of additional phases on MPB. Direct treatment of PB with $KMnO_4$ and HCl (i.e., BPB) resulted in precipitation of poorly crystalline birnessite as indicated by XRD peaks at d = 7.30 Å (001), 2.45 Å (100) and 1.42 Å (110) (Fig. S3a, Supporting information) (O'Reilly and Hochella, 2003).

TGA analysis indicates thermal stability of MPB is lower than BPB (Fig. 1). TGA curves include a relative stable phase and a rapid mass loss phase after combustion in the air. The main peak in response to the turning point for rapid weight loss appeared at 380 and 335 °C for PB and MPB respectively. This trend is contrary to that of the magnesium oxide, clay, and hematite modified biochars (Wang et al., 2015; Yao et al., 2013, 2014), where modified biochars have higher thermal stability than pristine biochar. This may be related to the transition of Mn-oxides during heating process in air atmosphere. Thermal transformation and TG characteristics of different Mn oxides under inert and air atmosphere had been studied in the literature (Gonzalez et al., 1996); and the authors found that manganite (MnOOH) and pyrolusite (MnO_2) exhibited faster weight loss at air, inert and reducing atmosphere,

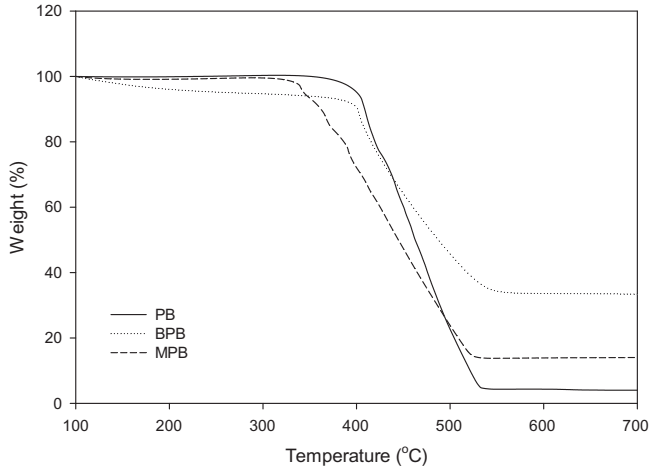

Fig. 1. Thermogravimetric (TG) curves of pine wood biochar (PB), $MnCl_2{\cdot}4H_2O$ modified biochar (MPB) and biochar modified with synthesized birnessite (BPB).

e.g., weight loss start from around 60 °C, and rapid weight loss start from below 300 and 600 °C under inert atmosphere, respectively. It is possible that some Mn oxides in MPB underwent transformation resulting in lower thermal stability. The weight of BPB did not maintain stable at the beginning as that of PB and MPB, instead it kept dropping, with lower slope in the first period and faster slope in the second period (Fig. 1). The relationship between weight and temperature showed a negative slope (R^2 = 0.92) until around 400 °C. This gradual weight loss in the first period of the BPB may be due largely to the water loss entrapped in the interlayers of birnessite (Gonzalez et al., 1996; Post, 1999). The better thermal stability of BPB may be related to the properties of birnessite, which is relatively stable until 620 °C in air atmosphere (Gonzalez et al., 1996).

3.2. As(V) and Pb(II) sorption kinetics and isotherms

As(V) and Pb(II) sorption by both composites as well as the pristine biochar was biphasic, with a rapid initial phase over the first few hours followed by a much slow sorption phase (Fig. 2). The rapid sorption phase may be ascribed to the rapid occupation of easily accessible external surface sorption sites, likely via physical sorption (Ahmad et al., 2014; Mohan et al., 2014). For example, rapid sorption kinetics were reported for As(V) sorption by Fe-modified activated carbon (Payne and Abel-Fattah, 2005) and for Pb(II) sorption between adjacent layers (not interlayers) of birnessite (O'Reilly and Hochella, 2003). The slow sorption phase may be attributed to specific (chemo-) and irreversible sorption (Ahmad et al., 2014; Mohan et al., 2014).

The sorption kinetics data was fitted with pseudo-first-order, pseudo-second order, and Elovich kinetic models (details of the models can be found in the supporting information) to provide insight into the potential sorption mechanisms (Fig. 2). As(V) sorption by PB, MPB and BPB was best-fit by the Elovich kinetic model with $R^2 > 0.98$ (Table S1). This was also true for Pb(II) sorption kinetics of the PB and MPB. For the BPB, however, the Pb(II) sorption kinetics were better described by the first and second order kinetic equations (Table S2). These results suggested that sorption of heavy metals on the biochar samples used in this work might be controlled by multiple mechanisms.

Based on the results of the Elovich model, the initial adsorption rate (α) of As(V) of MPB and BPB were more than 72.3 and 2.5 times greater than that of PB, respectively. For Pb(II), α of MPB and BPB was 18.3 and 41.3 times greater than that of PB, respectively. The As(V) and Pb(II) desorption constant (β) of MPB and BPB was also much lower than that of PB. These results indicated that, in comparison to the pristine biochar, the modified biochars had greater affinity to the two metals.

The sorption isotherms were generated by varying the ratio of sorbate to sorbent. At low sorbate concentrations (below about 5 mg kg^{-1} As(V) or Pb(II)), sorption isotherms increased rapidly with increasing equilibrium sorbate concentrations (Fig. 3). Sorption increased much more slowly at higher sorbate concentrations. Both Langmuir and Freundlich models reproduced the As(V) sorption isotherm data well ($R^2 > 0.98$, Table S1). The Langmuir maximum sorption capacities (S_{max}) of MPB and BPB to As(V) were

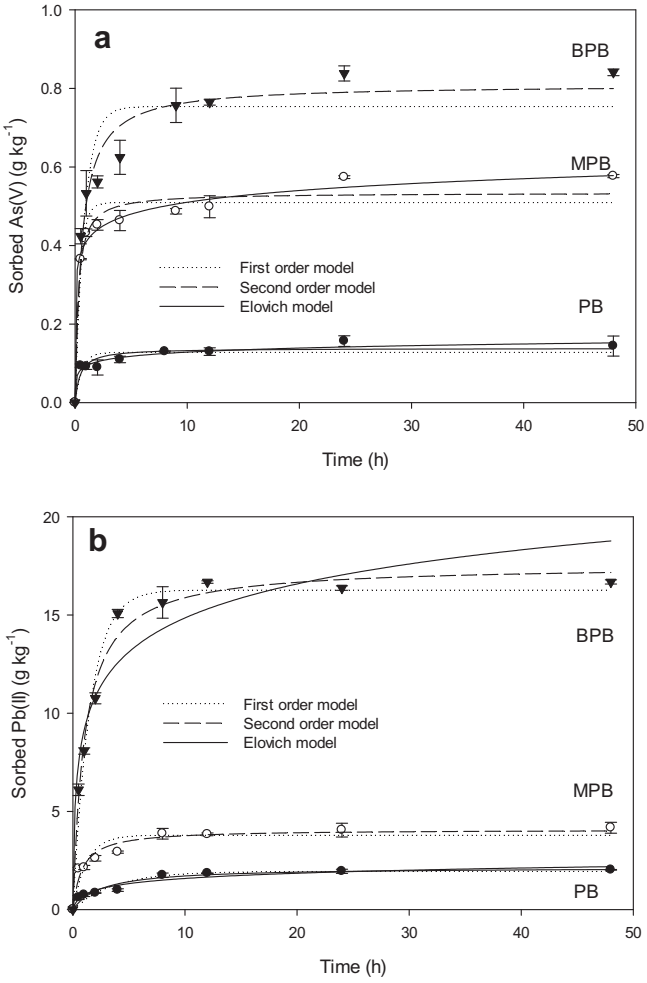

Fig. 2. As(V) (a) and Pb(II) (b) sorption kinetics data and fitted models for pine wood biochar (PB), $MnCl_2{\cdot}4H_2O$ modified biochar (MPB) and biochar modified with synthesized birnessite (BPB).

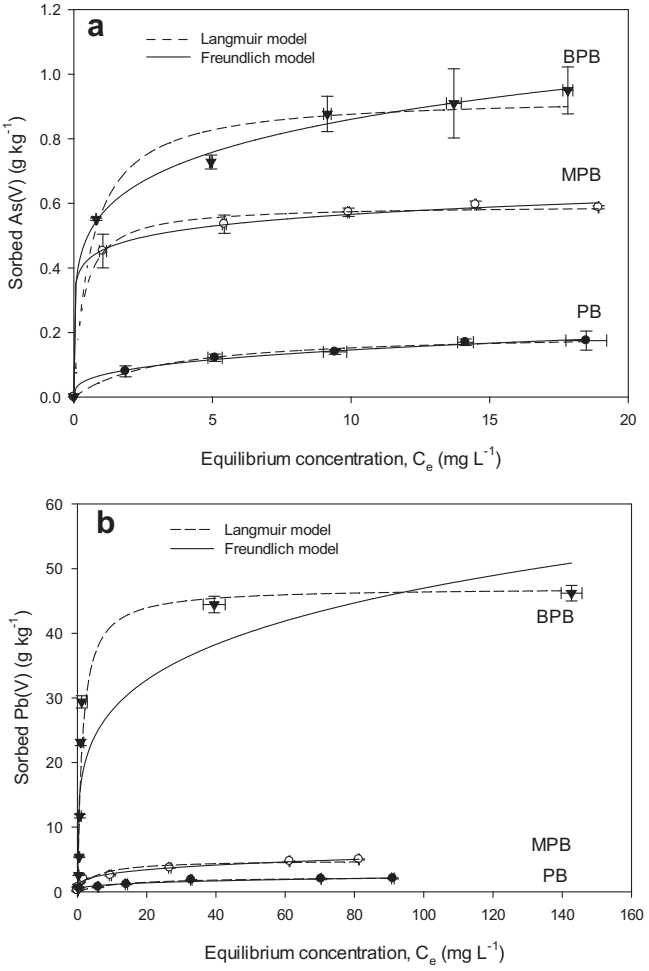

Fig. 3. As(V) (a) and Pb(II) (b) sorption isotherm data and fitted models for pine wood biochar (PB), $MnCl_2{\cdot}4H_2O$ modified biochar (MPB) and biochar modified with synthesized birnessite (BPB).

about 3.0 and 4.7 times greater than that of PB, respectively. Similarly, both the Langmuir and Freundlich models described the sorption of Pb(II) to the sorbents well (Table S2). The S_{max} of MPB and BPB to Pb(II) were about 2.1 and 20.0 times greater than that of PB, respectively. These results confirmed that the modification enhanced the As(V) and Pb(II) sorption ability of the biochar. The maximum Pb(II) and As(V) sorption capacities of the modified biochars, particularly BPB, are comparable to that of many other commonly used adsorbents reported in the literature (Tables S3 and S4).

3.3. As(V) sorption mechanisms

For the MPB, the EDS spectra of the post-sorption samples did not show the interaction between sorbed As(V) and Mn oxide (mainly MnO) particles (Fig. S4a and b, Supporting information), which might be because the content of As adsorbed on the MPB was below the determination limit of EDS (Hu et al., 2015). The XRD pattern of the post-sorption MPB (Fig. S2b, Supporting information) were similar to the original sample (Fig. S2a), suggesting precipitation might not play an important role in As sorption. Additional investigations are still needed to better understand the effects of MnO modification on the sorption of As(V) onto MPB.

Association of As(V) to Mn oxide (mainly birnessite) particles of post-sorption BPB samples was detected by the EDS analysis (Fig. S4c and d, Supporting information). This result indicated that interaction between As(V) and birnessite particles could play an important role in As(V) sorption onto the BPB. The XRD pattern of the post-sorption BPB (Fig. S3c, Supporting information) did not show any new peaks, suggesting precipitation might not be an important mechanism for As(V) sorption onto the BPB. Previous studies have demonstrated the strong interaction between As(V) and birnessite particles and the sorption is found to be related to edge site of birnessite (Manning et al., 2002; Tournassat et al., 2002).

3.4. Pb(II) sorption mechanisms

Similarly, the SEM/EDS analyses of the post-sorption MPB samples could not verify that the sorbed Pb(II) was related to the MnO particles in the MPB (Figs. S5 and S6, Supporting information). However, the SEM/EDS results of the post-sorption BPB showed the Pb(II) might be associated with the birnessite particles in the BPB (Fig. S7, Supporting information). This result suggested that birnessite particles in the modified biochars served as Pb(II) sorption site. The EDS mapping of the post-sorption MPB showed no obvious association of Pb(II) and MnO particles, but did show a large Pb particle (Figs. S6e and S5b, Supporting information), suggesting the precipitation mechanism (Inyang et al., 2012). This mechanism was further confirmed by comparing the XRD spectra of the MPB before and after Pb(II) sorption (Fig. S2, Supporting

information). XRD spectra of the post-sorption MPB showed new peaks at d = 3.597 and 3.409 Å (Fig. S2C, Supporting information), corresponding to Pb-bearing particles.

The XRD spectra of the post-sorption BPB did not show new peaks, suggesting precipitation might not be an important mechanism for Pb(II) sorption onto BPB. The EDS mapping of the post-sorption BPB (Fig. S7, Supporting information), however, showed some association between sorbed Pb(II) and the birnessite particles in the BPB. Previous studies have suggested that Pb(II) cations are sorbed either through diffusion into birnessite interlayers (O'Reilly and Hochella, 2003), by replacing cations located above or below the vacancy sites of birnessite (Lee et al., 2013), or by coordination to vacancy sites of hexagonal birnessite surface structure (Lafferty et al., 2010b; Matocha et al., 2001).

4. Conclusions

Biochar/manganosite (i.e., MPB) and biochar/birnessite (i.e., BPB) composites were synthesized. In comparison to the pristine biochar, although both MPB and BPB showed enhanced sorption of As(V) and Pb(II), the BPB had much better sorption ability. The enhanced As(V) and Pb(II) sorption by BPB was mainly due to the presences of birnessite particles within the BPB, which showed strong interactions with the two heavy metals and thus played an important role in the sorption. Findings from this work suggested that birnessite modification of biochar provides an effective way to prepare low-cost carbon adsorbents for heavy metal treatment.

Acknowledgement

This research was partially supported by the NSF (CBET-1054405) and STDF (Project 3804).

Appendix A. Supplementary data

Supplementary data associated with this article can be found, in the online version, at http://dx.doi.org/10.1016/j.biortech.2015.01.044.

References

Ahmad, M., Rajapaksha, A.U., Lim, J.E., Zhang, M., Bolan, N., Mohan, D., Vithanage, M., Lee, S.S., Ok, Y.S., 2014. Biochar as a sorbent for contaminant management in soil and water: a review. Chemosphere 99, 19–33.

Chen, L., Xing, H., Shen, Y., Bai, J., Jiang, G., 2009. Solid-state thermolysis of $[MnO]_{12}$ containing molecular clusters into novel MnO nano- and microparticles. J. Solid State Chem. 182 (6), 1387–1395.

Essington, M., 2004. Soil and Water Chemistry – An Integrative Approach. CRC Press.

Gonzalez, C., Gutierrez, J.I., GonzalezVelasco, J.R., Cid, A., Arranz, A., Arranz, J.F., 1996. Transformations of manganese oxides under different thermal conditions. J. Therm. Anal. 47 (1), 93–102.

Hu, X., Ding, Z., Zimmerman, A.R., Wang, S., Gao, B., 2015. Batch and column sorption of arsenic onto iron-impregnated biochar synthesized through hydrolysis. Water Res. 68, 206–216.

Inyang, M., Gao, B., Pullammanappallil, P., Ding, W., Zimmerman, A.R., 2010. Biochar from anaerobically digested sugarcane bagasse. Bioresour. Technol. 101 (22), 8868–8872.

Inyang, M., Gao, B., Yao, Y., Xue, Y., Zimmerman, A.R., Pullammanappallil, P., Cao, X., 2012. Removal of heavy metals from aqueous solution by biochars derived from anaerobically digested biomass. Bioresour. Technol. 110, 50–56.

Inyang, M.D., Gao, B., Ding, W.C., Pullammanappallil, P., Zimmerman, A.R., Cao, X.D., 2011. Enhanced lead sorption by biochar derived from anaerobically digested sugarcane bagasse. Sep. Sci. Technol. 46 (12), 1950–1956.

Lafferty, B., Ginder-Vogel, M., Sparks, D., 2010a. Arsenite oxidation by a poorly crystalline manganese-oxide 1. Stirred-flow experiments. Environ. Sci. Technol. 44 (22), 8460–8466.

Lafferty, B.J., Ginder-Vogel, M., Zhu, M.Q., Livi, K.J.T., Sparks, D.L., 2010b. Arsenite oxidation by a poorly crystalline manganese-oxide. 2. Results from X-ray absorption spectroscopy and X-ray diffraction. Environ. Sci. Technol. 44 (22), 8467–8472.

Lee, C.-Y., Kim, T., Komarneni, S., Han, S.-K., Cho, Y., 2013. Sorption characteristics of lead cations on microporous organo-birnessite. Appl. Clay Sci. 83–84, 263–269.

Lehmann, J., Gaunt, J., Rondon, M., 2006. Bio-char sequestration in terrestrial ecosystems – a review. Mitigation Adapt. Strateg. Global Change 11, 403–427.

Lenoble, W., Laclautre, C., Serpaud, B., Deluchat, V., Bollinger, J.C., 2004. As(V) retention and As(III) simultaneous oxidation and removal on a MnO_2-loaded polystyrene resin. Sci. Total Environ. 326 (1–3), 197–207.

Manning, B.A., Fendorf, S.E., Bostick, B., Suarez, D.L., 2002. Arsenic(III) oxidation and arsenic(V) adsorption reactions on synthetic birnessite. Environ. Sci. Technol. 36 (5), 976–981.

Matocha, C.J., Elzinga, E.J., Sparks, D.L., 2001. Reactivity of Pb(II) at the Mn(III,IV) (oxyhydr)oxide − water interface. Environ. Sci. Technol. 35 (14), 2967–2972.

McKenzie, R.M., 1980. The adsorption of lead and other heavy metals on oxides of manganese and iron. Aust. J. Soil Res. 18, 61–73.

Mohan, D., Pittman Jr., C.U., Bricka, M., Smith, F., Yancey, B., Mohammad, J., Steele, P.H., Alexandre-Franco, M.F., Gómez-Serrano, V., Gong, H., 2007. Sorption of arsenic, cadmium, and lead by chars produced from fast pyrolysis of wood and bark during bio-oil production. J. Colloid Interface Sci. 310 (1), 57–73.

Mohan, D., Sarswat, A., Ok, Y.S., Pittman Jr., C.U., 2014. Organic and inorganic contaminants removal from water with biochar, a renewable, low cost and sustainable adsorbent – a critical review. Bioresour. Technol. 160, 191–202.

O'Reilly, S.E., Hochella Jr., M.F., 2003. Lead sorption efficiencies of natural and synthetic Mn and Fe-oxides. Geochim. Cosmochim. Acta 67 (23), 4471–4487.

Payne, K., Abel-Fattah, T., 2005. Adsorption of arsenate and arsenite by iron-treated activated carbon and zeolites: effects of pH, temperature, and ionic strength. J. Environ. Sci. Health. Part A 40 (4), 723–749.

Post, J., 1999. Manganese oxide minerals: crystal structures and economic and environmental significance. Proc. Natl. Acad. Sci. U. S. A. 96 (7), 3447–3454.

Sun, Y., Gao, B., Yao, Y., Fang, J., Zhang, M., Zhou, Y., Chen, H., Yang, L., 2014. Effects of feedstock type, production method, and pyrolysis temperature on biochar and hydrochar properties. Chem. Eng. J. 240, 574–578.

Tournassat, C., Charlet, L., Bosbach, D., Manceau, A., 2002. Arsenic(III) oxidation by birnessite and precipitation of manganese(II) arsenate. Environ. Sci. Technol. 36 (3), 493–500.

Wang, S., Gao, B., Zimmerman, A., Li, Y., Ma, L., Harris, W., Migliaccio, K., 2015. Removal of arsenic by magnetic biochar prepared from pinewood and natural hematite. Bioresour. Technol. 175, 391–395.

Yao, Y., Gao, B., Chen, J.J., Zhang, M., Inyang, M., Li, Y.C., Alva, A., Yang, L.Y., 2013. Engineered carbon (biochar) prepared by direct pyrolysis of Mg-accumulated tomato tissues: characterization and phosphate removal potential. Bioresour. Technol. 138, 8–13.

Yao, Y., Gao, B., Fang, J., Zhang, M., Chen, H., Zhou, Y., Creamer, A., Sun, Y., Yang, L., 2014. Characterization and environmental applications of clay–biochar composites. Chem. Eng. J. 242, 136–143.

Zhang, M., Gao, B., Varnoosfaderani, S., Hebard, A., Yao, Y., Inyang, M., 2013. Preparation and characterization of a novel magnetic biochar for arsenic removal. Bioresour. Technol. 130, 457–462.

Zhang, S., Niu, H., Cai, Y., Zhao, X., Shi, Y., 2010. Arsenite and arsenate adsorption on coprecipitated bimetal oxide magnetic nanomaterials: $MnFe_2O_4$ and $CoFe_2O_4$. Chem. Eng. J. 158 (3), 599–607.

Zhang, T., Sun, D.D., 2013. Removal of arsenic from water using multifunctional micro-/nano-structured MnO_2 spheres and microfiltration. Chem. Eng. J. 225, 271–279.

Zhou, Y., Gao, B., Zimmerman, A.R., Chen, H., Zhang, M., Cao, X.D., 2014. Biochar-supported zerovalent iron for removal of various contaminants from aqueous solutions. Bioresour. Technol. 152, 538–542.